

Supplementary Materials

ZMYND8 expression in breast cancer cells blocks T-lymphocyte surveillance to promote tumor growth

Yong Wang,^{1‡} Maowu Luo,^{1‡} Yan Chen,¹ Yijie Wang,¹ Bo Zhang,¹ Zhenhua Ren,¹ Lei Bao,¹ Yanan Wang,¹ Jennifer E. Wang,¹ Yang-Xin Fu,¹ Weibo Luo,^{1,2*} and Yingfei Wang^{1,3*}

¹Department of Pathology,

²Department of Pharmacology,

³Department of Neurology,

UT Southwestern Medical Center, Dallas, TX 75390, USA.

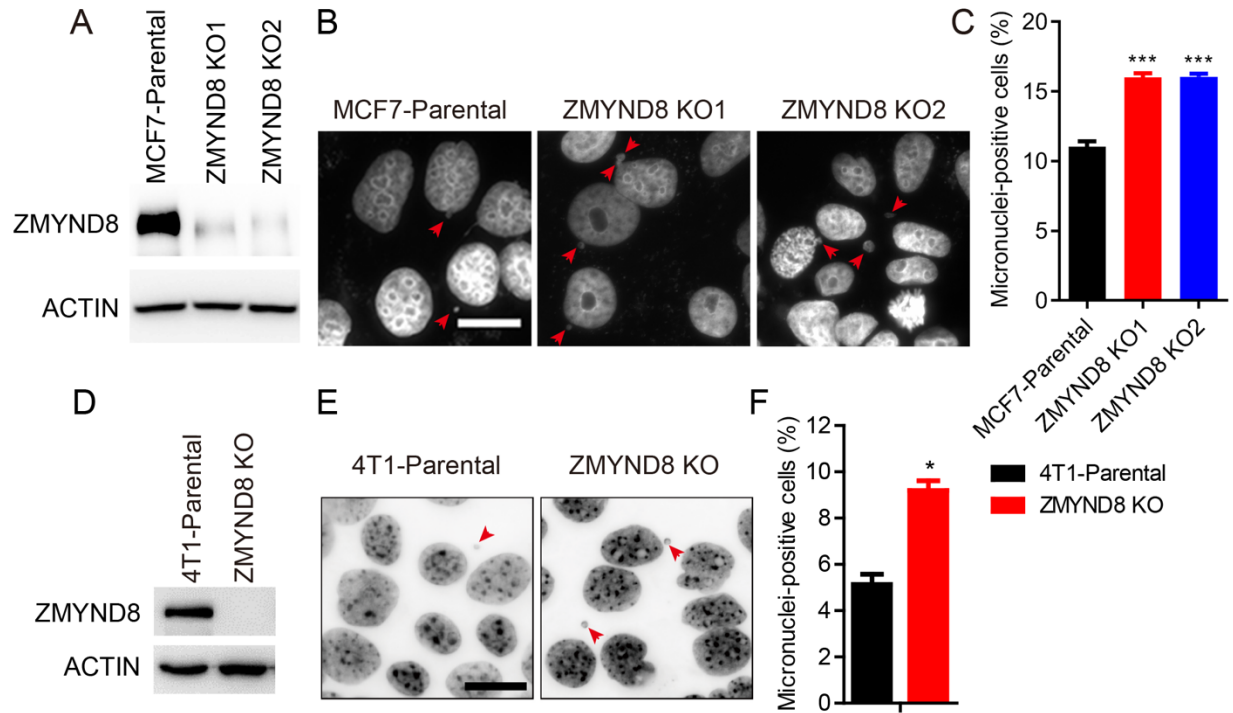
Supplementary Table 1. The sgRNA Sequences

| Target genes | Sequences | Target location |
|-----------------|----------------------------|-----------------|
| mouse ZMYND8 #1 | 5'-GCAGTTGTGCAGGATCCACT-3' | exon 8 |
| mouse ZMYND8 #2 | 5'-CGGGTTTATCACGCTAAGTG-3' | exon 5 |
| mouse cGAS #1 | 5'-CCGAGGCGCGGAAAGTCGTA-3' | exon 1 |
| mouse cGAS #2 | 5'-AAAGGGGGGCTCGATCGCGG-3' | exon 1 |
| mouse STING #1 | 5'-GATGATCCTTTGGGTGGCAA-3' | exon 1 |
| mouse STING #2 | 5'-GTTGAAAAACCTCTGCTGTC-3' | exon 3 |
| mouse P65 #1 | 5'-ATCGAACAGCCGAAGCAACG-3' | exon 3 |
| SC | 5'-ACGGAGGCTAAGCGTCGCAA-3' | |

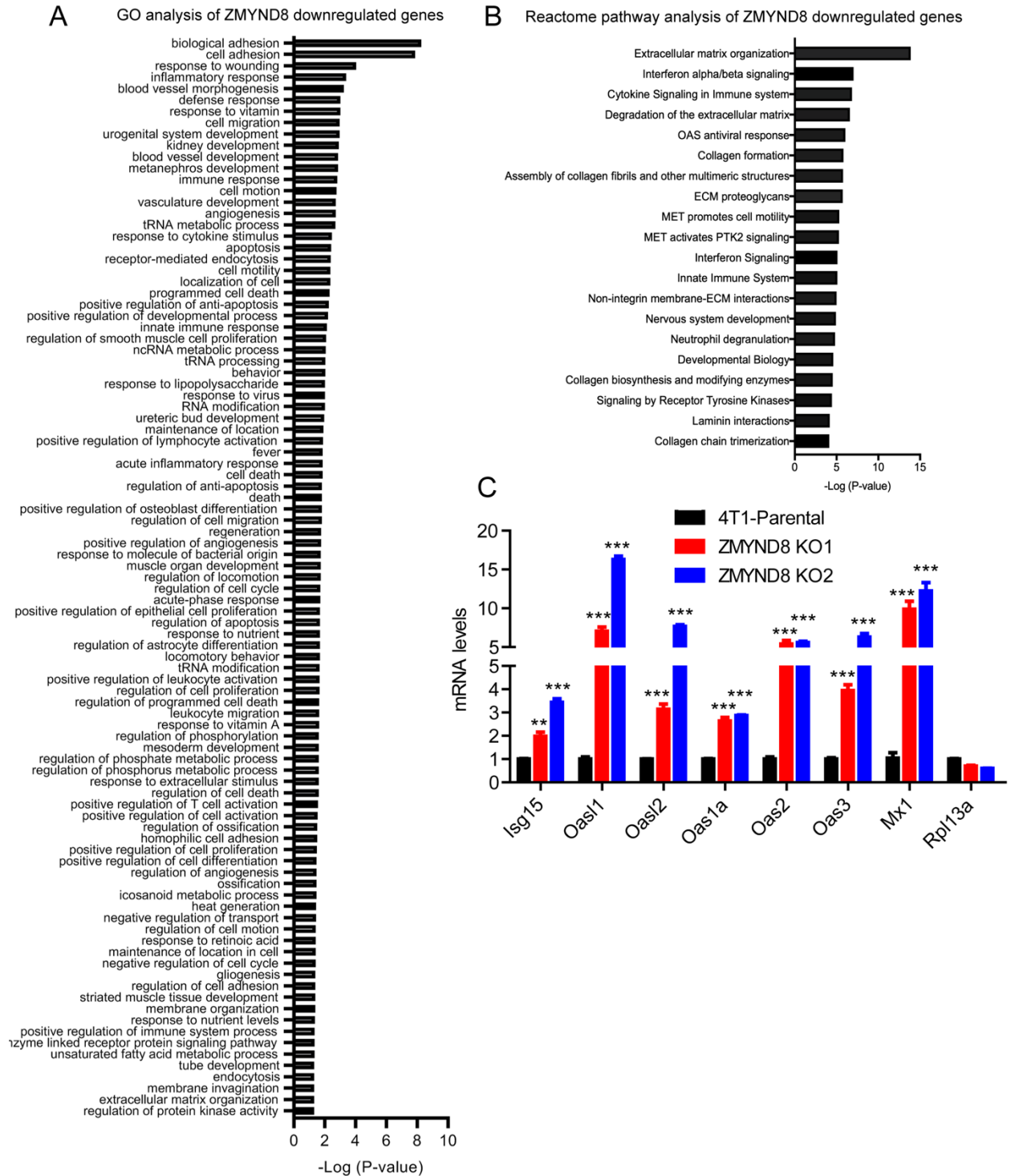
Supplementary Table 2. qPCR Primers

| | |
|---------------------------------|--|
| human IFN- β (RT-qPCR) | Forward: 5'-ATGACCAACAAGTGTCTCCTCC-3' |
| | Reverse: 5'-GGAATCCAAGCAAGTTGTAGCTC-3' |
| human ISG15 (RT-qPCR) | Forward: 5'-ACTCATCTTTGCCAGTACAGG-3' |
| | Reverse: 5'-CAGCTCTGACACCGACATG-3' |
| human OSAL (RT-qPCR) | Forward: 5'-GTGGCAGAAGGGTACAGATG-3' |
| | Reverse: 5'-CTGTCAAGTGGATGTCTCGTG-3' |
| human OAS1 (RT-qPCR) | Forward: 5'-CATCTGTGGGTTCTGAAGG-3' |
| | Reverse: 5'-GAGAGGACTGAGGAAGACAAC-3' |
| human OAS2 (RT-qPCR) | Forward: 5'-GTTATCCTCTCCCTGCTTCAAG-3' |
| | Reverse: 5'-GGATTCTATGGCTTCTGGATGAG-3' |
| human RPL13A (RT-qPCR) | Forward: 5'-CTCAAGGTCGTGCGTCTG-3' |
| | Reverse: 5'-TGGCTTTCTCTTTCCTCTTCTC-3' |
| human 18S rRNA (RT-qPCR) | Forward: 5'-CGGCGACGACCCATTCGAAC-3' |
| | Reverse: 5'-GAATCGAACCTGATTCCCCGTC-3' |
| mouse Ifn- β (RT-qPCR) | Forward: 5'-AGCTCCAAGAAAGGACGAACA-3' |
| | Reverse: 5'-GCCCTGTAGGTGAGGTTGAT-3' |
| mouse Isg15 (RT-qPCR) | Forward: 5'-CCCAGTGCACAGTGATCAAG-3' |
| | Reverse: 5'-TCCAATGCTATCCCAAAGTCC-3' |
| mouse Oas11 (RT-qPCR) | Forward: 5'-CTGTATCTACTGGACCAAGCAC-3' |
| | Reverse: 5'-GCCACTATGTCCCATCTGTAG-3' |
| mouse Oas12 (RT-qPCR) | Forward: 5'-ATCATTGTCCTTACCCACAGAG-3' |
| | Reverse: 5'-TGCTGGTTTTGAGTCTCTGG-3' |
| mouse Oas1a (RT-qPCR) | Forward: 5'-AGAGATGCTTCCAAGGTGC-3' |
| | Reverse: 5'-ACTGATCCTCAAAGCTGGTG-3' |
| mouse Oas2 (RT-qPCR) | Forward: 5'-GCCTGAATACTGAGTCACCTG-3' |
| | Reverse: 5'-TTCAGTAAGTGGCTTGGAGTG-3' |
| mouse Oas3 (RT-qPCR) | Forward: 5'-TGCTACTGGTCAAACACTGG-3' |
| | Reverse: 5'-CTGAACTTTTGCTCTCCACAG-3' |

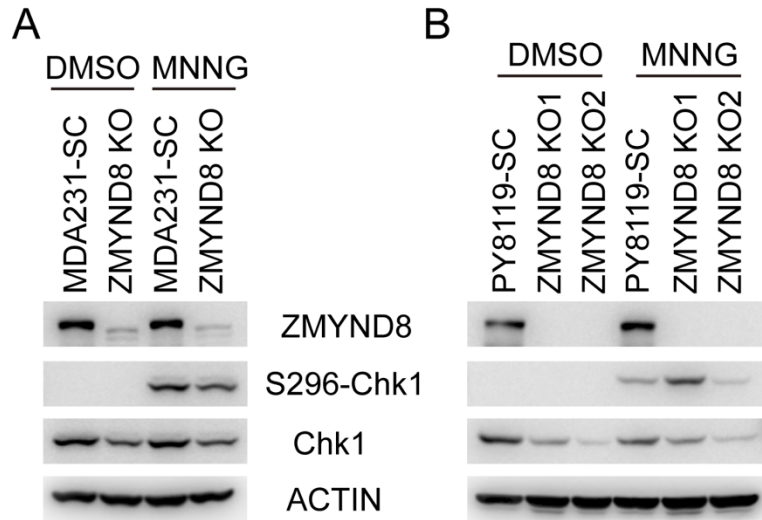
| | |
|----------------------------|---|
| mouse Mx1 (RT-qPCR) | Forward: 5'-GACCATAGGGGTCTTGACCAA-3' |
| | Reverse: 5'-AGACTTGCTCTTTCTGAAAAGCC-3' |
| mouse Cxcl10 (RT-qPCR) | Forward: 5'-TCAGCACCATGAACCCAAG-3' |
| | Reverse: 5'-CTATGGCCCTCATTCTCACTG-3' |
| mouse Rpl13a (RT-qPCR) | Forward: 5'-GGGCAGGTTCTGGTATTGGAT-3' |
| | Reverse: 5'-GGCTCGGAAATGGTAGGGG-3' |
| mouse Actin (RT-qPCR) | Forward: 5'-GGCTGTATTCCCCTCCATCG-3' |
| | Reverse: 5'-CCAGTTGGTAACAATGCCATGT-3' |
| mouse Ifnb1 (ChIP-qPCR) | Forward: 5'-ATTCCTCTGAGGCAGAAAGGACCA-3' |
| | Reverse: 5'-GCAAGATGAGGCAAAGGCTGTCAA-3' |
| mouse Isg15 (ChIP-qPCR) | Forward: 5'-CCTTTCCTTCCCAACTACAG-3' |
| | Reverse: 5'-TTCCAGAAACCAGAGCTATTT-3' |
| mouse Oas2 (ChIP-qPCR) | Forward: 5'-GCTAGCTGGAAGCAAACA-3' |
| | Reverse: 5'-GAAAGAGGAAATCAAGTCCAAAG-3' |
| mouse Oas3 (ChIP-qPCR) | Forward: 5'-GGAGACAGCAGAACCATAAA-3' |
| | Reverse: 5'-GTCACCTCCCTTCACTTTC-3' |
| mouse Mx1 (ChIP-qPCR) | Forward: 5'-CGGTTTCAATTCTCCTCTGG-3' |
| | Reverse: 5'-CTGTGCAATACTCACCCTC-3' |



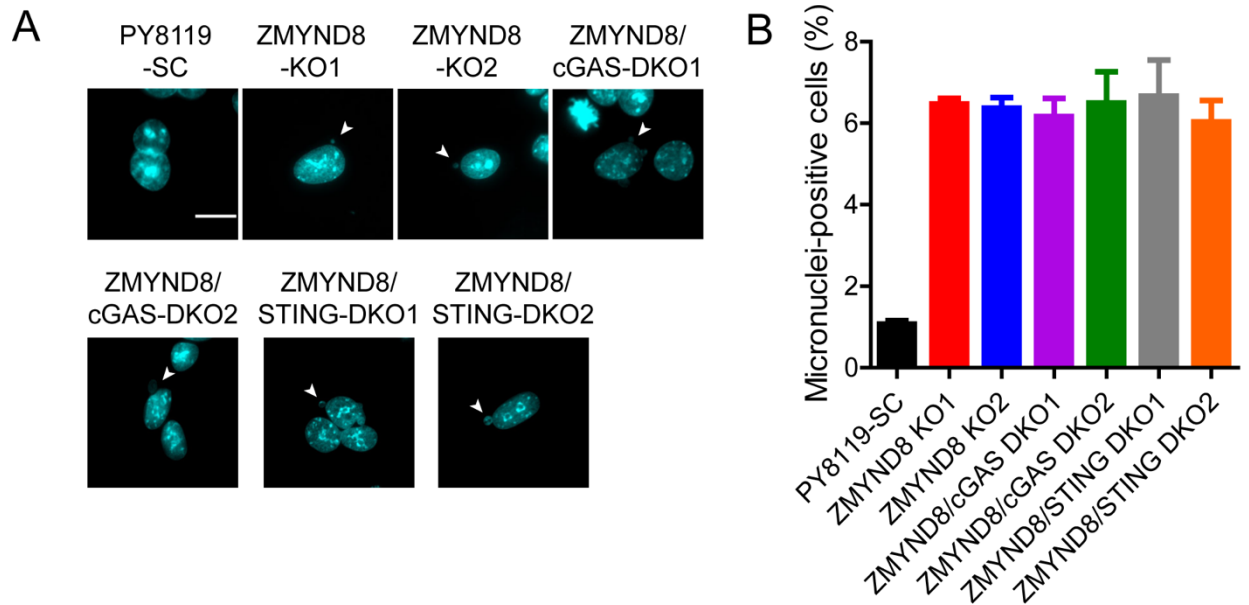
Supplementary Figure 1. ZMYND8 KO increases micronucleus formation in breast cancer cells. (A) Immunoblot analysis of ZMYND8 and actin in parental, ZMYND8 KO1, and ZMYND8 KO2 MCF-7 cells. (B) Representative images of micronuclei (indicated by red arrows) in parental, ZMYND8 KO1, and ZMYND8 KO2 MCF-7 cells. Scale bar, 10 μ m. (C) Quantification of the number of micronuclei in parental, ZMYND8 KO1, and ZMYND8 KO2 MCF-7 cells ($n = 200-300$, mean \pm SEM). *** $p < 0.001$ vs. MCF-7 by one-way ANOVA with Dunnett's test. (D) Immunoblot analysis of ZMYND8 and actin in parental and ZMYND8 KO 4T1 cells. (E) Representative images of micronuclei (indicated by red arrows) in parental and ZMYND8 KO 4T1 cells. Scale bar, 10 μ m. (F) Quantification of the number of micronuclei in parental and ZMYND8 KO 4T1 cells ($n = 458-521$, mean \pm SEM). * $p < 0.05$ vs. 4T1 by Student's t test.



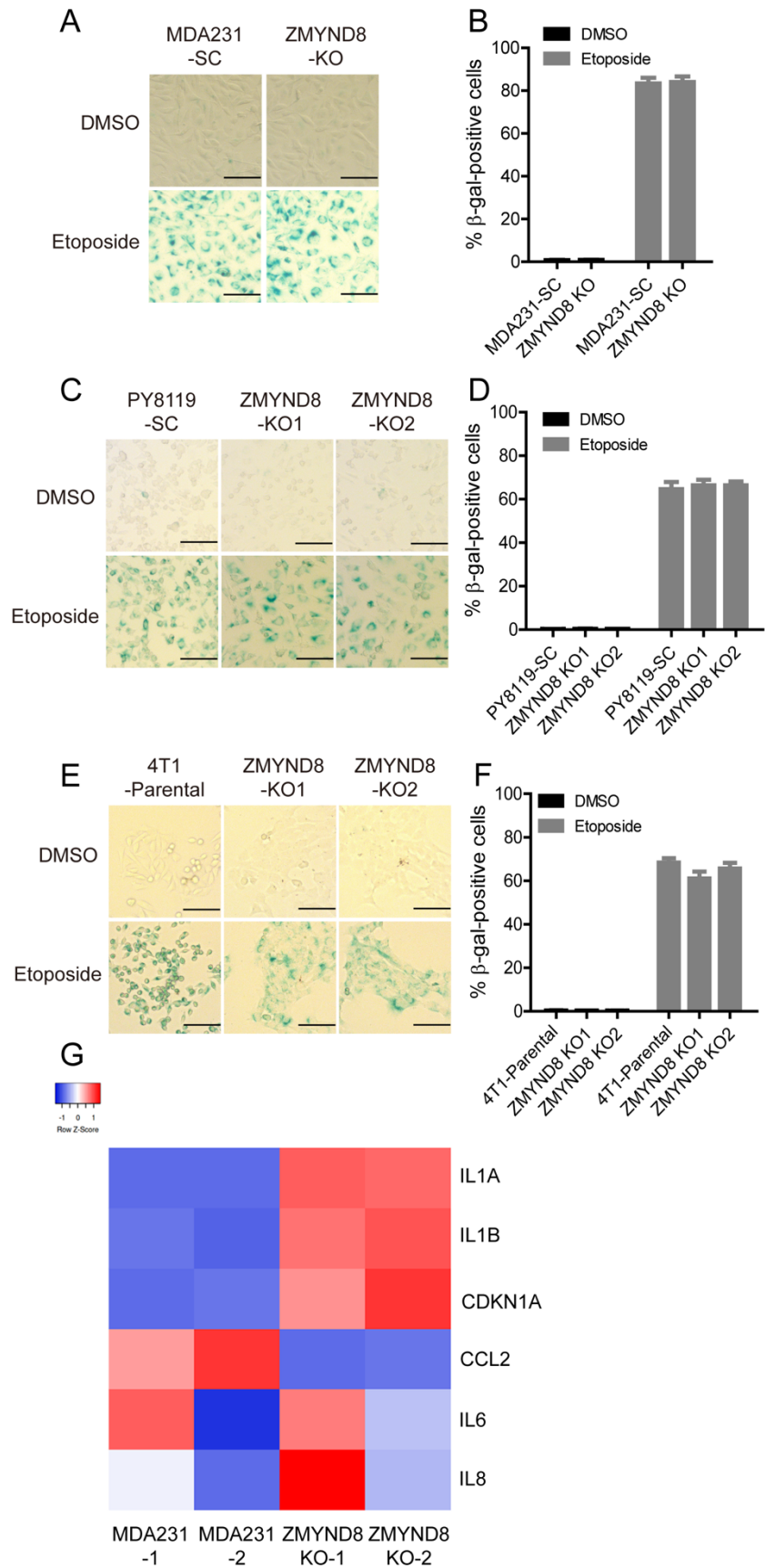
Supplementary Figure 2. ZMYND8 suppresses ISGs in breast cancer cells. (A) GO analysis of ZMYND8-downregulated genes. (B) Reactome pathway analysis of ZMYND8-downregulated genes. Top 20 pathways are shown. (C) RT-qPCR analysis of ISGs and Rpl13a mRNAs in SC, ZMYND8 KO1, and ZMYND8 KO2 4T1 cells ($n = 3$, mean \pm SEM). ** $p < 0.01$; *** $p < 0.001$ vs. SC by one-way ANOVA with Dunnett's test.



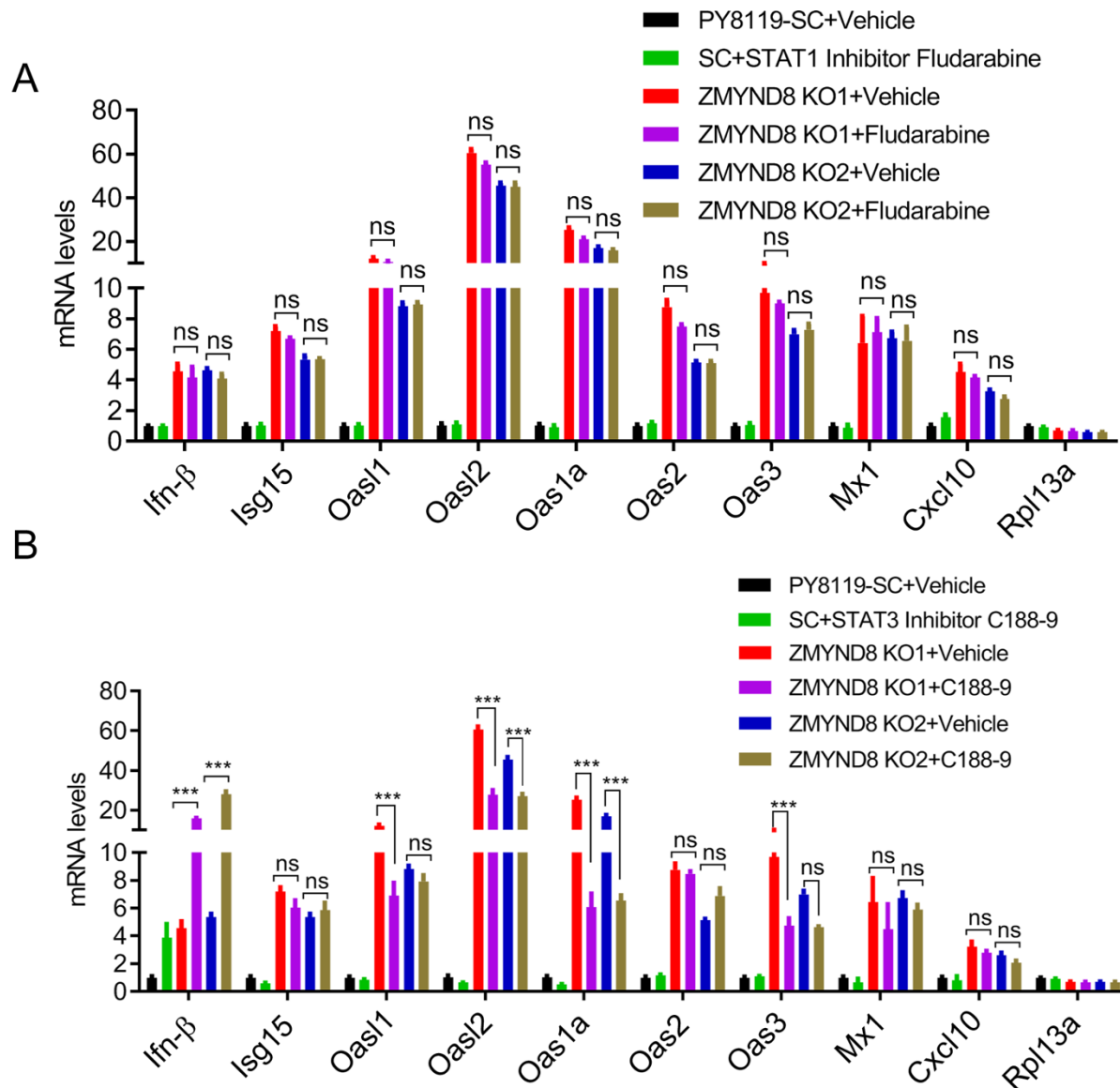
Supplementary Figure 3. ZMYND8 loss fails to induce the cell-cycle checkpoint response in breast cancer cells. SC and ZMYND8 KO MDA-MB-231 (MDA231, **A**) and PY8119 (**B**) cells were treated with DMSO or MNNG (75 μ M) for 15 min and then incubated for additional 4 hours. Immunoblot assay was performed with indicated antibodies. Representative immunoblots from two independent experiments are shown.



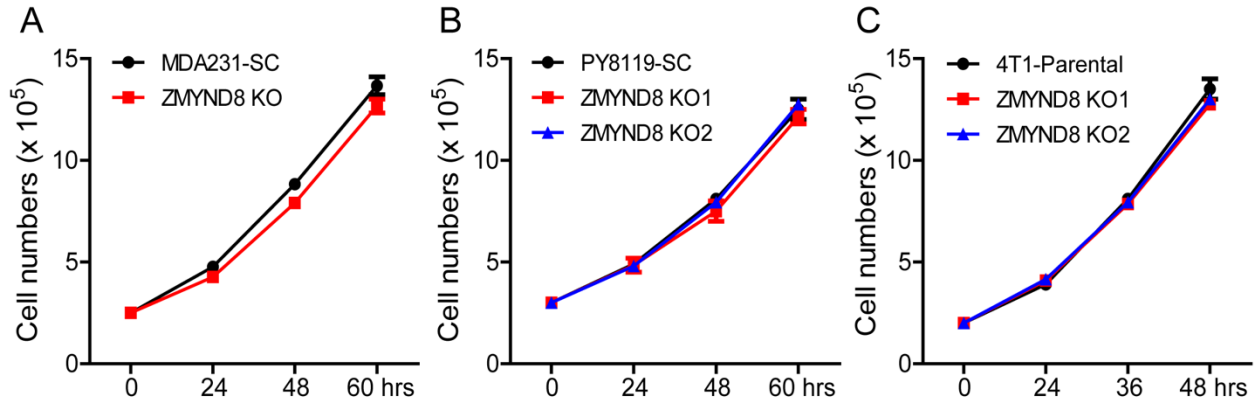
Supplementary Figure 4. Deletion of cGAS or STING does not lead to a further increase of micronuclei in ZMYND8 KO cells. (A) Representative immunostaining of micronuclei in SC, ZMYND8 KO1, ZMYND8 KO2, ZMYND8/cGAS DKO1, ZMYND8/cGAS DKO2, ZMYND8/STING DKO1, and ZMYND8/STING DKO2 PY8119 cells. Scale bar, 10 μ m. (B) Quantification of micronuclei in SC, ZMYND8 KO1, ZMYND8 KO2, ZMYND8/cGAS DKO1, ZMYND8/cGAS DKO2, ZMYND8/STING DKO1, and ZMYND8/STING DKO2 PY8119 cells ($n = 300$, mean \pm SEM).



Supplementary Figure 5. ZMYND8 loss fails to induce senescence in breast cancer cells. (A-F) SC/parental and ZMYND8 KO MDA-MB-231 (MDA231, **A** and **B**), PY8119 (**C** and **D**), and 4T1 (**E** and **F**) cells were treated with DMSO or etoposide (12.5 μ M) for 24 hours and subjected to senescence-associated β -galactosidase assay. Representative images are shown in **A**, **C**, and **E**. The percentage of β -galactosidase (gal)-positive cells is quantified in **B**, **D**, and **F** ($n = 3$, mean \pm SEM). Scale bar, 10 μ m. (**G**) The heatmap of senescence-associated gene expression in parental and ZMYND8 KO MDA-MB-231 cells. Gene expression data were retrieved from RNA-seq (GSE108833).



Supplementary Figure 6. STAT1 and STAT3 are not involved in ZMYND8 KO-induced IFN- β and ISGs expression in PY8119 cells. (A) SC, ZMYND8 KO1, and ZMYND8 KO2 PY8119 cells were treated with a STAT1 inhibitor Fludarabine or vehicle for 24 hours, and subjected to RT-qPCR analysis of IFN- β , ISGs, and Rpl13a mRNAs ($n = 3$, mean \pm SEM). ns, not significant. (B) SC, ZMYND8 KO1, and ZMYND8 KO2 PY8119 cells were treated with a STAT3 inhibitor C188-9 or vehicle for 24 hours, and subjected to RT-qPCR analysis of IFN- β , ISGs, and Rpl13a mRNAs ($n = 3$, mean \pm SEM). *** $p < 0.001$ by two-way ANOVA with Tukey's test.



Supplementary Figure 7. ZMYND8 loss has no effect on cell proliferation *in vitro*. SC or parental and ZMYND8 KO MDA-MB-231 (MDA231, **A**), PY8119 (**B**), and 4T1 (**C**) cells were subjected to *in vitro* cell growth assay using trypan blue 24, 48, and 60 hours after culture. Data are shown in mean \pm SEM (n = 3).